

ROBUST CEREBROVASCULAR SEGMENTATION IN 4D ASL MRA IMAGES

Renzo Phellan* Thomas Linder† Michael Helle‡ Alexandre X. Falcão§ Nils D. Forkert**

* Biomedical Engineering Graduate Program, University of Calgary
2500 University Drive NW, Calgary, AB, Canada

† Clinic for Radiology and Neuroradiology, University medical center Schleswig-Holstein
Kiel, Germany

‡ Philips Technologie GmbH, Innovative Technologies, Hamburg, Germany

§ Laboratory of Image Data Science, Institute of Computing, University of Campinas
Campinas, SP, Brazil

** Department of Radiology and Hotchkiss Brains Institute, University of Calgary
Calgary, AB, Canada

ABSTRACT

Cerebrovascular diseases are one of the main causes of disability and death in the world. Methods for segmentation of the cerebral blood vessels can help clinicians to visualize the cerebrovascular system, determine age-related normal values, and diagnose and study cerebrovascular diseases. A common problem for these methods is the precise delineation of small vessels, due to different artifacts depending on the medical imaging modality. In this work, we present an automatic segmentation method for four dimensional arterial spin labeling magnetic resonance angiography (4D ASL MRA) images of the brain, which allows an improved segmentation of small vessels, reaching an average Dice similarity coefficient (DSC) of 0.946 based on an evaluation of five datasets from healthy subjects. The results show that the proposed method is able to account for the magnetic labeling decay and flow related artifacts, which considerably reduce the contrast of small vessels present in the image, leading to improved segmentation results.

Index Terms— Angiography, vessel segmentation, arterial spin labeling.

1. INTRODUCTION

Cerebrovascular diseases, such as aneurysms, arteriovenous malformations, stenoses, and strokes, are one of the main causes of disability and death in the world, according to the world health organization [1]. Four dimensional arterial spin labeling magnetic resonance angiography (4D ASL MRA) is a non-invasive imaging modality, which allows to simultaneously display the morphology of the vessels in the brain as well as blood flow dynamics. It can help clinicians and researchers to study the cerebrovascular system, determine age-related normal values, and diagnose and study cerebrovascu-

lar diseases [2]. 4D ASL MRA relies on magnetic labeling of the blood to increase the contrast of the vessels, thus, avoiding the injection of exogenous contrast agents to the patient, and exposure to ionizing radiation, as it is required in case of other modalities used to study the cerebrovascular system, which can potentially cause allergic reactions or cancer [3].

4D ASL MRA is acquired as a set of pairs of 3D images, with high temporal resolution, while blood flows through the brain. Each pair comprises one control image, and one image containing magnetically labeled blood at a specific time point. When both images of a pair are subtracted, most of the non-vascular tissues are removed, so that vessels appear more clearly (see Figure 1). Nevertheless, the residual noise after subtraction represents a challenge for segmentation and visualization, as it can present signal intensities similar to those of small vessels [4], making its removal a complex task. Additionally, 4D ASL MRA generates a considerable amount of data, which is tedious to analyze directly, and limits its application in the clinical practice. Automatic segmentation methods can be used to process the data contained in 4D ASL MRA and present relevant information to the user. Nevertheless, current methods for vessel segmentation fail to accurately segment 4D ASL MRA partly due to magnetic labeling decay, as the altered magnetic state of labeled blood gradually returns to its initial state, and flow related artifacts, which considerably reduce the contrast of small vessels present in the image, making their signal intensity comparable to that of residual noise [4].

This present paper describes a robust segmentation method for cerebrovascular segmentation in 4D ASL MRA images. It includes algorithms that recover small vessels, which are especially affected by magnetic labeling decay and flow related artifacts, and it also removes residual noise after subtraction of control and labeled image pairs, by analyzing blood flow data. The new method represents an improvement in accuracy

with respect to our previous approach described in [5].

2. MATERIALS

In order to evaluate our method, we use five 4D ASL MRA sequences acquired from healthy volunteers. These series were obtained at the University Medical Center Schleswig-Holstein Campus Kiel, Germany, with approval of the local ethics committee.

A Philips Achieva 3T MRI machine (Philips Healthcare, Best, The Netherlands) was used to obtain the series of 4D ASL MRA images. Each 4D ASL MRA image series contains five control/labeled image pairs, with a temporal resolution of 120 ms. Each image contains 120 slices with 224×224 voxels and voxel size of $0.94 \times 0.94 \times 1.0$ mm³. Additional acquisition parameters are: T1-Turbo Field Echo (TFE) scan with a TFE factor of 16, SENSE factor: 3, TR/TE: 7.7/3.7 ms, flip angle: 10°, half scan factor: 0.7, and 5 minutes scan time.

In the same session, 3D multi-slab time-of-flight magnetic resonance angiography (TOF MRA) images were also acquired from the same five volunteers. Each TOF-MRA images contains 171 slices with 512×512 voxels and voxel size of $0.41 \times 0.41 \times 0.70$ mm³. Additional acquisition parameters are: SENSE factor: 2, TR/TE: 20/3.45 ms, flip angle: 20°, 3 slabs, flow compensated readout, and 6:39 minutes scan time.

3. METHODS

3.1. Preprocessing

Each image of the 4D ASL MRA series is initially filtered using the denoising algorithm proposed by Coupe et al. [6], which reduces noise while preserving edges and small structures of interest, such as vessels. After that, corresponding control/labeled pairs of images are subtracted to remove tissues that do not belong to vessels. Figure 1 shows three control/labeled pairs of images of a 4D ASL MRA series, at different time points ($t = 440, 680$, and 920 ms), and the result after subtraction, which still contains residual noise from non-vascular tissues.

In the last preprocessing step, the multiscale vesselness filter according to the formulation of Erdt et al. [7] is applied to the images that result from subtraction. This filter enhances tubular-shaped structures in the image, such as vessels, and it has been shown to be beneficial to increase the accuracy of the final segmentation [8].

3.2. Segmentation

Each one of the five images of a 4D ASL MRA series, resulting from subtraction, is used as input to the segmentation process described in the following. First, the voxels of the

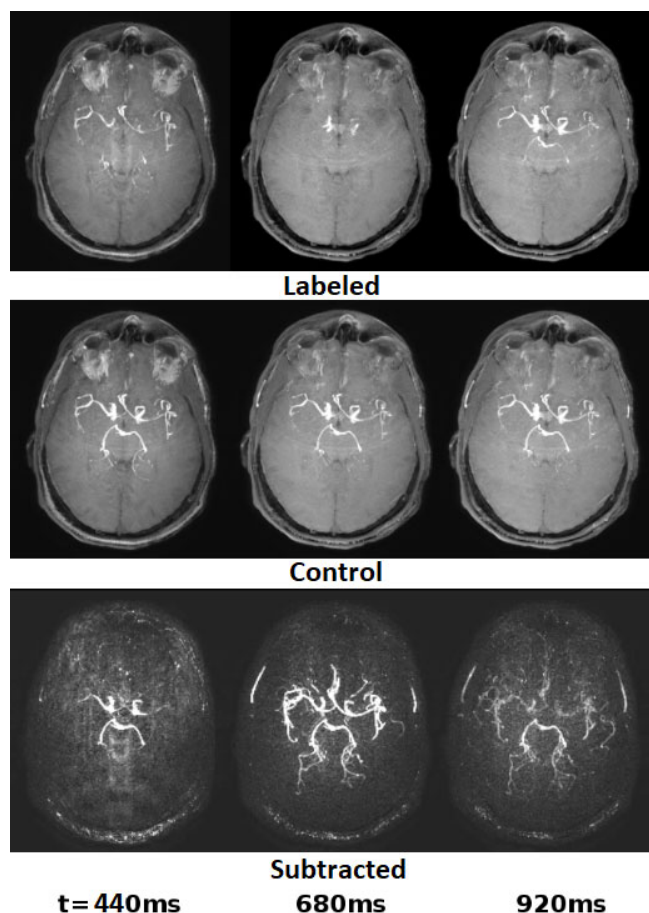


Fig. 1. Maximum intensity projections of 30 slices for three control/labeled image pairs of a 4D ASL MRA series, and their corresponding result after subtraction. The first row corresponds to labeled images, the second row to control images, and the third row to the result after subtraction. Notice the presence of residual noise in the images of the last row.

first vesselness image of a series are separated in two clusters (voxels that belong or not to vessel tissue) using the K-means algorithm.

Given that the initial image of a series usually contains only large vessels, and the magnetic labeling decay has not yet considerably affected the signal, the first K-means segmentation does not present gaps or low intensity vessels. Nevertheless, dispersion of the labeled blood, due to flow characteristics, may generate intensity variations along the vessels and in areas close to the vessel wall, which translate into false negatives in the K-means segmentation result.

In order to account for the dispersion effect, the K-means segmentation result is refined by using a level-set segmentation algorithm, according to the local formulation described by Lankton et al. [9]. This formulation evolves the front of the level-set by separating the average intensity values of voxels in the vessel and non-vessel classes, as proposed by Chan and

Vese [10], but only considering voxels inside a sphere of a fixed radius. As a consequence, the size of the sphere can be adjusted to contain vessel regions small enough not to present high intensity variations, leading to a more accurate level-set segmentation.

Finally, only the largest connected component is considered in the final segmentation, as the cerebrovascular system is assumed to be one connected component at any time point.

Once the first image of a series of five images is processed, the K-means and level-set algorithms are applied again to the second image. The binary segmentation of the first image is directly added to the second image segmentation using an OR operator. No considerable motion artifacts were noticed between images of the same series, due to the fact that the images were acquired from healthy volunteers. However, motion correction algorithms could be used to correct this possible problem [11].

Typically starting with the third image of a series with this specific temporal resolution, some other problems arise, which complicate the segmentation process. First, flow related artifacts generate gaps with low intensity values in the middle of the vessels that receive labeled blood from this time point and after. As a consequence, the K-means segmentations of the third, fourth, and fifth image also present gaps in the middle of vessel structures, which cannot be corrected by the level-set segmentation step. Second, as the signal intensity of small vessels decreases due to the magnetic labeling decay, the level-set segmentations of the third, fourth, and fifth images contain tubular-shaped structures, generated by residual noise with signal intensity comparable to that of small vessels, attached to the vascular tree that does not correspond to vessels.

The first problem, gaps in the middle of vessel structures, is solved by using the image foresting transform (IFT) algorithm [12]. This algorithm considers a connectivity function to add optimum paths of adjacent voxels of maximum signal intensity between disconnected segments of the same vessel. The path generated by the IFT has a thickness of only one voxel. To overcome this problem, its final thickness is calculated by linear interpolation between the values of the thickness of the segments it connects.

In order to deal with the second problem, non-vessel tubular structures attached to the vascular tree, the proposed segmentation method keeps track of which segments of the cerebrovascular system are identified at each time point. In doing so, only newly segmented structures that connect to regions of the cerebrovascular system segmented in the two previous timepoints are added to the final segmentation while structures not fulfilling this requirement are not added to the final segmentation.

Finally, the corrected segmentations of the third, fourth, and fifth images are sequentially added to the final segmentation as in the case of the first two images.

3.3. Evaluation

In order to create a reference for ground-truth segmentation, manual delineation is impractical and very laborious. As an alternative, a validated algorithm [13] is used to segment the vessels present in TOF MRA 3D images of the brain of the same healthy subjects. The TOF MRA images are then registered to the 4D ASL MRA images using the software Elastix [14], and the same transformations are applied to their corresponding binary segmentations. These registered segmentations were reviewed and manually corrected prior to be used as a reference for evaluation of the proposed method.

The Dice similarity coefficient (DSC) is used to compare the segmentations obtained with the method proposed in this paper and the reference segmentations. In order to account for possible registration errors, a tolerance margin of one voxel is considered for the calculation of the DSC score.

4. RESULTS AND DISCUSSION

The DSC values obtained when comparing the segmentations generated by the proposed method with the reference segmentations of the cerebrovascular system, for each of the five 4D ASL MRA series, are presented in Table 1. The proposed method reaches an average DSC value of 0.946, which is higher than the DSC value of 0.932 obtained in our previous work for the same five subjects [5].

Subject	DSC
1	0.951
2	0.916
3	0.944
4	0.962
5	0.958
Average	0.946
Standard deviation	0.018

Table 1. DSC values for the proposed segmentation method.

Figure 2 shows 3D visualizations of the reference segmentation and the result of the proposed segmentation algorithm for one 4D ASL MRA series. Here, it can be seen that the proposed method correctly identifies small vessels (indicated by red arrows).

The present work represents a first approach to combine anatomical and blood flow information, which are both included in the 4D ASL sequence, for improved cerebrovascular segmentation. Vesselness intensity values are used to guide the algorithms included in the proposed method, but they may be affected by the presence of residual noise. In this case, a continuous flow assumption is used to discard falsely identified vessel branches, such that branches that do not connect to vascular structures identified in the two immediately previous time points are discarded.

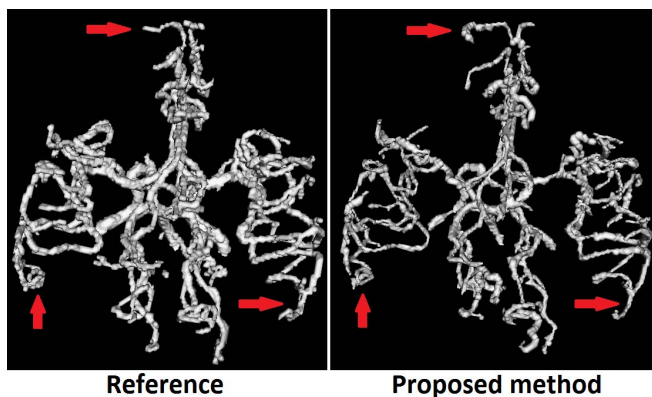


Fig. 2. 3D visualizations of reference and the proposed method vessel segmentations. Red arrows indicate correctly identified small vessels.

5. CONCLUSION

In conclusion, this paper presents a segmentation method for extraction of vessels of the brain in 4D ASL MRA images. A main benefit of the proposed method compared to previous approaches is that it can recover small vessels, with signal intensities affected by magnetic labeling decay and flow related artifacts. The segmentation results can be considered highly accurate, reaching an average DSC value of 0.946.

6. ACKNOWLEDGMENT

This work was supported by Natural Sciences and Engineering Research Council of Canada (NSERC) and Hotchkiss Brain Institute (HBI). Dr. Nils D. Forkert is funded by Canada Research Chairs. Dr. Alexandre X. Falcao thanks CNPq 302970/2014-2 and FAPESP 2014/12236-1.

7. REFERENCES

- [1] World Health Organization, "The top 10 causes of death," 2015.
- [2] Thomas W Okell, Michael A Chappell, Mark W Woolrich, Matthias Günther, David A Feinberg, and Peter Jezzard, "Vessel-encoded dynamic magnetic resonance angiography using arterial spin labeling," *Magnetic resonance in medicine*, vol. 64, no. 3, pp. 698–706, 2010.
- [3] Thomas Lindner, Ulf Jensen-Kondering, Matthias JP van Osch, Olav Jansen, and Michael Helle, "3D time-resolved vessel-selective angiography based on pseudo-continuous arterial spin labeling," *Magnetic resonance imaging*, vol. 33, no. 6, pp. 840–846, 2015.
- [4] Renzo Phellan, Thomas Lindner, Alexandre X Falcão, and Nils D Forkert, "Vessel segmentation in 4D arterial spin labeling magnetic resonance angiography images of the brain," in *SPIE medical imaging*. International society for optics and photonics, 2017, pp. 101341B–101341B.
- [5] Renzo Phellan, Thomas Lindner, Michael Helle, Alexandre Falcao, and Nils Daniel Forkert, "Automatic temporal segmentation of vessels of the brain using 4D ASL MRA images," *IEEE transactions on biomedical engineering*, 2017.
- [6] Pierrick Coupé, Pierre Yger, Sylvain Prima, Pierre Hellier, Charles Kervrann, and Christian Barillot, "An optimized blockwise nonlocal means denoising filter for 3D magnetic resonance images," *IEEE transactions on medical imaging*, vol. 27, no. 4, pp. 425–441, 2008.
- [7] Marius Erdt, Matthias Raspe, and Michael Suehling, "Automatic hepatic vessel segmentation using graphics hardware," *Medical imaging and augmented reality*, pp. 403–412, 2008.
- [8] Renzo Phellan and Nils D Forkert, "Comparison of vessel enhancement algorithms applied to Time-of-Flight MRA images for cerebrovascular segmentation," *Medical physics*, 2017.
- [9] Shawn Lankton and Allen Tannenbaum, "Localizing region-based active contours," *IEEE transactions on image processing*, vol. 17, no. 11, pp. 2029–2039, 2008.
- [10] Tony F Chan and Luminita A Vese, "Active contours without edges," *IEEE transactions on image processing*, vol. 10, no. 2, pp. 266–277, 2001.
- [11] Mark Jenkinson, Peter Bannister, Michael Brady, and Stephen Smith, "Improved optimization for the robust and accurate linear registration and motion correction of brain images," *Neuroimage*, vol. 17, no. 2, pp. 825–841, 2002.
- [12] Alexandre X Falcão, Jorge Stolfi, and Roberto de Alencar Lotufo, "The image foresting transform: Theory, algorithms, and applications," *IEEE transactions on pattern analysis and machine intelligence*, vol. 26, no. 1, pp. 19–29, 2004.
- [13] Nils Daniel Forkert, Alexander Schmidt-Richberg, Jens Fiehler, Till Illies, Dietmar Möller, Dennis Säring, Heinz Handels, and Jan Ehrhardt, "3D cerebrovascular segmentation combining fuzzy vessel enhancement and level-sets with anisotropic energy weights," *Magnetic resonance imaging*, vol. 31, no. 2, pp. 262–271, 2013.
- [14] Stefan Klein, Marius Staring, Keelin Murphy, Max A Viergever, and Josien PW Pluim, "Elastix: A toolbox for intensity-based medical image registration," *IEEE transactions on medical imaging*, vol. 29, no. 1, pp. 196–205, 2010.